Thermal design and performance of the SCUBA-2 instrument 1-K and mK systems

Adam L. Woodcraft*,[1,2] Matthew I. Hollister,[1] Dan Bintley,[3] Fred C. Gannaway,[4,†] David C. Gostick,[2] and Wayne S. Holland[2]

[1]*SUPA‡, Institute for Astronomy, University of Edinburgh, Blackford Hill, Edinburgh EH9 3HJ, UK*
[2]*UK Astronomy Technology Centre, Blackford Hill, Edinburgh EH9 3HJ, UK*
[3]*Joint Astronomy Centre, 660 N. A'ohoku Place, University Park, Hilo, Hawaii 96720 USA*
[4]*Cardiff School of Physics and Astronomy, Cardiff University, Queens Buildings, The Parade, Cardiff CF24 3AA, UK*

Various research fields require large and complex instruments containing detectors operating at millikelvin temperatures. The materials and techniques traditionally used in cryogenics are often unsuitable for the demanding requirements of such instruments. We describe the thermal design and performance of the 1-K and millikelvin systems of the SCUBA-2 instrument. This is an astronomical "camera" operating at wavelengths of 450 and 850 μm. It is the largest and most complex instrument ever built for sub-mm astronomy, and the first to use a cryogen-free dilution refrigerator. The design consists of a mix of traditional techniques (but used in demanding situations) as well as novel elements. The thermal performance has been stable and very successful, and we hope that the details described here will be useful to the designers of future large instruments.

Keywords: (D) Instrumentation (F) Cryostats (C) Thermal conductivity

1 Introduction

Various research fields such as astronomy [1] and fundamental physics [2] require large instruments containing detectors operating at millikelvin temperatures. The scale and demanding requirements of these instruments often require innovative design, as traditional techniques and materials used in smaller-scale experiments can be insufficient. One example is the SCUBA-2 [1] instrument on the James Clerk Maxwell Telescope in Hawaii. This is a "camera" operating at wavelengths of 450 and 850 μm, and is the largest and most complex instrument ever built for sub-mm astronomy.

Images are produced using over 10 000 transition edge superconducting (TES) detectors [3]. To meet the performance requirements, the detectors must be heat sunk at a temperature of around 60 mK and must be surrounded by radiation shielding at a temperature of approximately 1.5 K. The millikelvin and 1-K stages are cooled respectively by the mixing chamber and still of a cryogen-free dilution refrigerator (DR)[1].

The DR is located at a considerable distance (approximately a metre) from the detectors, requiring thermal links to transfer the cooling power. These links have several required properties which limit the achievable thermal conductance: they must have a degree of flexibility to permit motion during thermal contraction and demountable joints are required to permit components to be removed for repair or replacement. Another set of competing requirements arises from the need to rigidly support the detectors from the 1-K box while keeping the heat input to an acceptable level.

Despite these difficulties and the overall complexity, the thermal design has been highly successful, and met the requirements on the very first cooldown. This paper describes the design for the 1-K and millikelvin stages along with their performance. We pay particular attention to details of the design which are likely to be relevant to future instruments of similar (or greater) complexity. We also describe the rationale for various design decisions, in the hope that they will be useful to workers faced with similar problems. The overall design of the instrument, including the design of higher temperature stages, is described elsewhere [4].

2 Design

2.1 Overview

The SCUBA-2 instrument contains two focal planes so that it can perform simultaneous imaging at two wavelengths (450 and 850 μm). Each focal plane is made up of four detectors, called subarrays, each of which consists of bonded silicon wafers with dimensions approximately 40 × 50 mm. The purpose of the instrument is to maintain the detectors at their operating temperature, to support them mechanically in a precise position, to bring the image from the telescope onto the detectors, to block other sources of radiation, and to provide magnetic shielding from the telescope environment.

Each of the eight sub-array detectors is contained in a subarray module, shown in the top right hand corner in Fig. 1. This contains the detectors as well as the cryogenic read-out circuitry. To achieve the required sensitivity the detectors must operate at millikelvin temperatures, but the final cryogenic readout stage, consisting of series arrays of 100 SQUIDS, must operate at the 1-K temperature stage as the power dissipation is too high for the millikelvin stage to handle. A subarray module therefore contains sections held at two different temperatures.

The four sub-array modules in each focal plane are contained within a focal plane unit (FPU), shown in Fig. 1. The two FPUs provide thermal and electrical interfaces to the sub-array modules, as well as optical and magnetic shielding. Electrical connections are provided via multi-pin MDM connectors, while bolted joints form thermal and mechanical interfaces. A filter in each FPU permits radiation of the required wavelengths to enter and thus reach the detectors, while rejecting all other wavelengths.

The FPUs are contained within an enclosure called the 1-K box, shown in Fig. 2. This supports the FPUs and the thermal links running between them and the dilution refrigerator insert.

*E-mail: adam.woodcraft@physics.org. Tel.: +44-870-765-1873; Fax: + 44-870-879-7873
‡Scottish Universities Physics Alliance
†Current address: Department of Physics, Queen Mary, University of London, Mile End Road, London E1 4NS, UK
[1] Leiden Cryogenics BV, Leiden, Netherlands

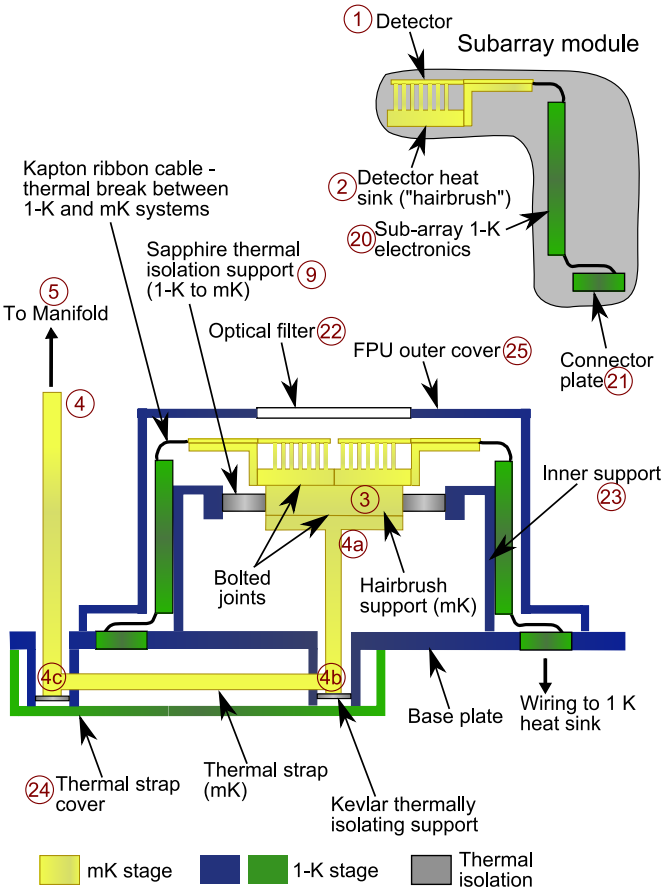

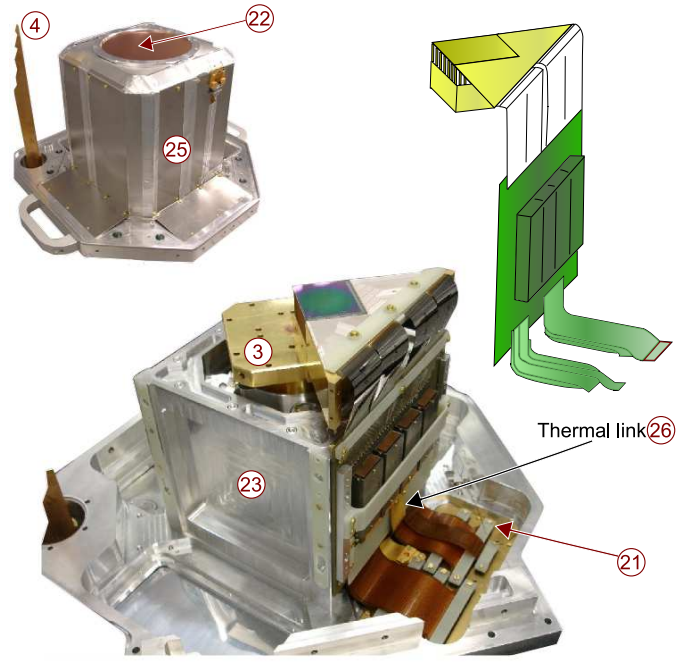

Figure 1: (Top group) Cross-sectional schematic (not to scale) of a focal plane unit (FPU), showing two out of the four subarray modules contained within. A single subarray module is shown in the grey area in the top right hand corner. (Bottom group) Image of an FPU with a single subarray module installed, and (top left) with the FPU outer cover in place. The numbers denoting the different components are the same for all figures in the paper.

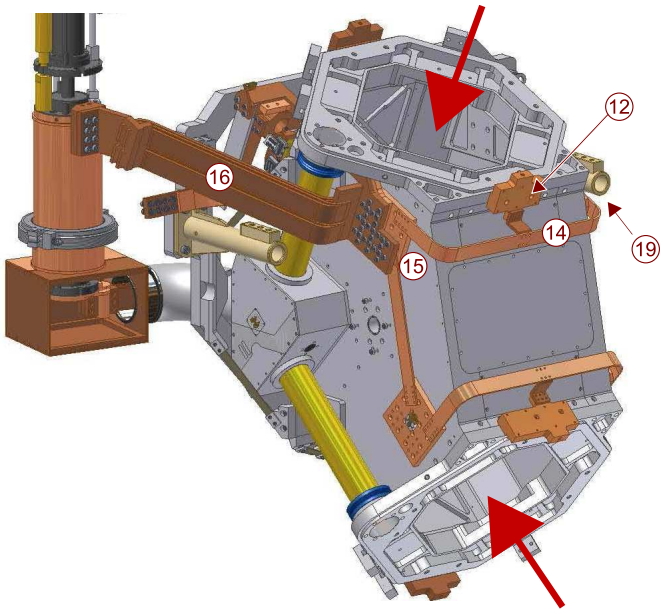

Figure 2: CAD image of the 1-K box, without the FPUs installed. The thick arrows show the direction in which the FPUs are inserted. The numbered components are: heat sinking plates (12,19), copper thermal links (14,16) and the "epoxy joint" (15). These are described in the text and in Fig. 5.

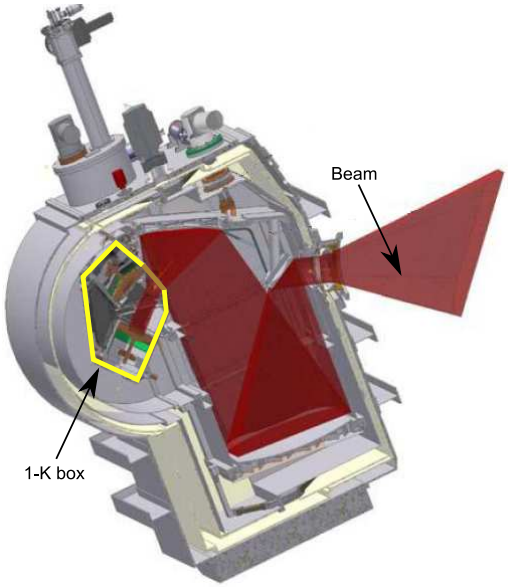

Figure 3: The SCUBA-2 cryostat, showing the location of the 1-K box. Most of the space inside the cryostat is required for the optical beam.

The 1-K box also provides further magnetic and optical shielding, and contains a dichroic (beamsplitter) which feeds the signal from the sky onto the two focal planes. The FPUs can be removed from the 1-K box; the sub-array modules can then be removed and replaced independently. Figure 3 shows how the 1-K box fits into the overall instrument, and Fig. 4 shows a picture of the 1-K box installed in the instrument with all the array wiring in place.

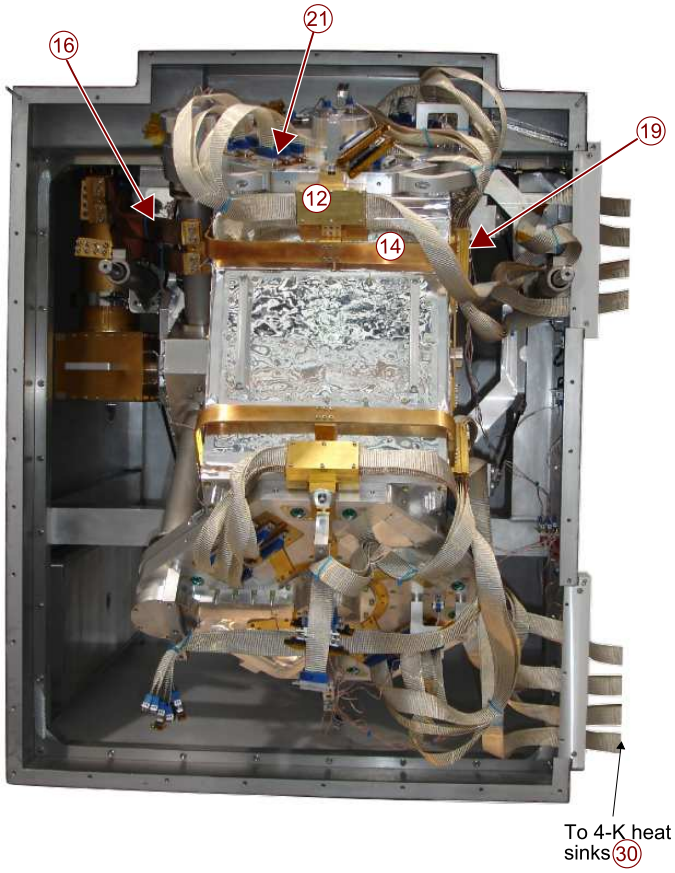

Figure 4: Photograph of the 1-K box installed in the SCUBA-2 cryostat. The numbered components are: heat sinking plates (12,19), copper thermal links (14,16) and a connector plate (21).

A constraint on the design is that we avoided ferromagnetic materials within the 1-K box due to the possibility of magnetic interference with the SQUIDs in the detector read-out circuitry.

The 1-K box is cooled by the still of the dilution refrigerator. This is necessary because the "dry" (cryocooler precooled) dilution refrigerator lacks the 1-K pot of a traditional fridge which would normally be used to provide cooling power. Copper thermal links run between the still and the 1-K box. A separate system of copper links runs between the mixing chamber of the dilution fridge and the millikelvin stage of the FPUs; these are entirely enclosed by radiation shielding at a temperature of approximately 1.5 K. Wiring to the arrays is made by Monel clad niobium titanium, woven into ribbon cables. In total there are over 2000 wires, and each ribbon cable is heat sunk at the 60-K, 4-K and 1-K stages before reaching the arrays. The thermal layout of the 1-K box and the FPUs is shown in Fig. 5. The critical areas of the thermal design are described in more detail in the following sections.

2.2 1-K stage

The 1-K stage must completely surround the detectors to prevent black-body radiation and stray-light from reaching the them. The 1-K box is constructed from aluminium alloy (6082 T6). Aluminium alloy was chosen since it has a low density, minimizing the mass of the instrument, and is readily machined. This particular alloy was chosen as it was available in suitable sizes, and has a higher thermal conductivity than the majority of aluminium alloys [5] while maintaining reasonable mechanical properties. To make

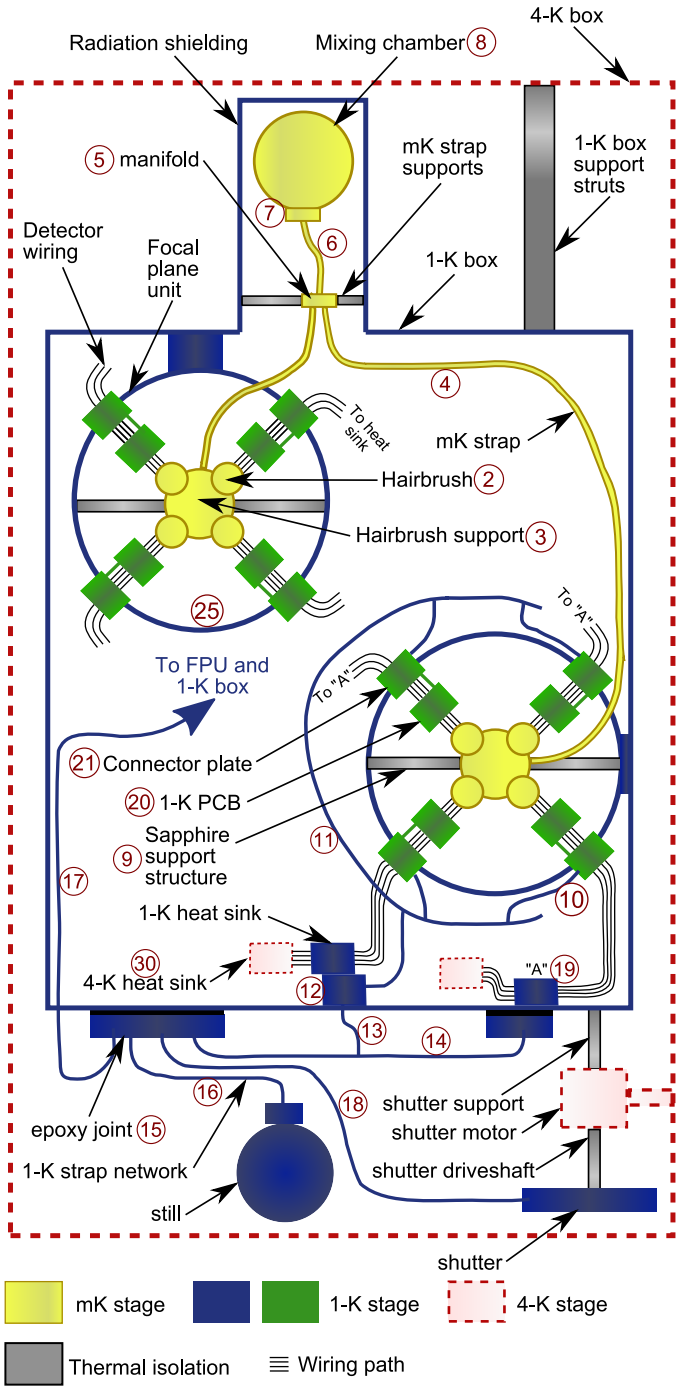

Figure 5: The thermal layout of the 1-K and mK stages. For simplicity, the 1-K links are only shown linking to the connector plates on one of the focal plane units.

manufacture practical, the box is constructed from several sections bolted together. Once assembled, there is no requirement for disassembly, and to improve thermal conduction across the bolted joints they were bonded together with Stycast[2] 2850 FT epoxy (the choice of expoxy is discussed later in this section).

To reduce black-body radiation on the detectors to an acceptable level, the maximum temperature of the box should be

[2] Emerson & Cuming, Billerica, MA, USA

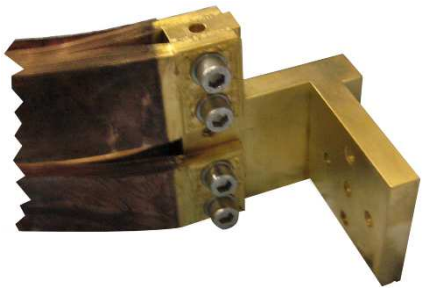

Figure 6: Photograph of one end of the thermal link between the still and the 1-K box. The millikelvin thermal links are similar, except that they are gold plated throughout and the weld is not supplemented with bolts.

1.5 K. However, this temperature would give an unacceptably high *conductive* load down wiring and the supports to the millikelvin stage. We therefore aimed to maintain an upper temperature of 1.1 K at the appropriate points (this was later relaxed to 1.3 K as described in section 3).

We did not wish to rely on thermal conduction through the 1-K box to achieve this, since aluminium alloys are relatively poor thermal conductors and the conduction across the bolted joints is unknown. Instead, a system of copper thermal links provide an all-copper path from the dilution refrigerator still to both sides of the box, the heat sinks for the detector wiring and to the base of each FPU; these can be seen in Fig. 2 and are shown schematically in Fig. 5 (components 10–18).

At these temperatures, temperature drops at bolted joints are significant, and can dominate the overall temperature drop across a thermal link. Careful attention was paid to the design of the joints, in particular designing them to allow a large contact force [6]. The most risky joints are those which must be broken apart and re-made during the life of the instrument (for example to remove the dilution fridge insert for repair), as there is the possibility of degradation of performance over time or due to mishandling. The number of such joints was kept to a minimum. In principle, the remaining joints could have been made by welding or in some other permanent fashion to improve conductance. However, modelling showed that there was sufficient margin in the expected thermal performance that further bolted joints could be used to simplify assembly. Since copper is easily deformed, in order to be able to repeatedly make the joints in a reliable fashion, helicoils were used in all the copper tapped holes. The screws were A2 non-magnetic stainless steel.

Thermal contact from the still of the dilution fridge to the 1-K box is made via flexible links consisting of stacks of 0.1 mm thick vacuum annealed 5N (99.999%) purity copper foil with commercial copper (ETP, electrolytic tough pitch) end pieces. The foils are diffusion bonded at each end to give a solid cross-section which is then electron beam welded into the end pieces. Annealing and using such high purity copper provides improved thermal conductivity compared with using standard commercial copper, while using thin foils provides flexibility to allow for movement during thermal contraction. A further reason to use foils is that we have found it relatively easy to procure 5N copper in the form of thin foils, but not in bulk form.

The use of ETP copper end-pieces has little impact on the overall conductance of the links, and has the advantage that it is less soft than 5N copper, which would be likely to deform significantly after repeated make and break cycles. The ends were gold plated; the straps were too long to conveniently gold plate the entire length, and the main purpose of the gold plating is to prevent oxidation of the bolted surfaces. Inspection of these straps after welding gave us some concern about the weld quality, and the welded interface was therefore supplemented with M6 bolts as a precaution.

The link consists of four parallel stacks of 50 foils, each with a total cross-section of 160 mm^2; a photograph of one end is shown in Fig. 6. The length is 410 mm. This link carries all the heat flowing from the 1-K stage, and is the limiting factor on the cool-down time of the 1-K box. It was therefore designed for higher performance than the rest of the 1-K thermal links. The minimum number of bolted contacts for this link would be two (one at each end), but for assembly reasons a further bolted joint at the still was necessary. Two M8 bolts were used for one joint at the still and eight M6 bolts (at a torque of 9 Nm) for the other.

Making good thermal contact to aluminium is difficult because of the poorly conducting oxide layer which forms. Gold plating aluminium without trapping an oxide layer under the plating is not straightforward, particularly for large aluminium structures. A further concern is degradation of such a joint due to differential thermal contraction between aluminium and copper on repeated cooldowns. Overall, we could not justify a test programme to determine if we could make sufficiently good contact to the 1-K box with a metal to metal joint. Instead, the straps are bolted to a large area copper plate, which is itself glued and bolted to the side of the 1-K box. While the conduction through epoxy is much lower than for a good metal to metal contact, such a joint has a large effective contact area since the epoxy flows into irregularities in the surfaces, whereas contact in a pure metal to metal joint is made over a much smaller area than the nominal contact area. The conduction through an epoxy joint is therefore easier to predict as it does not depend significantly on joint pressure and surface properties, and is thus less of a risk than a bolted joint. The copper plate is 10 mm thick, and has an area of 100 mm $\times$ 100 mm. The epoxy used was Stycast 1266. A filled epoxy such as Stycast 2850 FT would have had a better thermal contraction match to aluminium and therefore have been more suitable; 1266 was used in error, but the thermal and mechanical performance has been satisfactory. Five M5 bolts were used at a torque of 6 Nm for the bolted joint between the 1-K strap and the copper plate. Ideally only one joint would be broken to remove the 1-K box from the instrument, but in practice the 1-K link is unbolted at both ends since it is too heavy to be safely left unsupported.

As seen in Figs. 2 and 5, the copper plate (component 15) acts as a junction for a network of further thermal links. As these links carry less heat than the main thermal link, it was possible to make these from ETP copper, and to use smaller cross-sections and bolted joints. The links had a width of 25 mm and a thickness of 3 mm, and the bolted joints were generally made with six M4 screws at a torque of 2 Nm. Two links (components 14 and 17 in Fig. 5) run to further copper plates epoxied and bolted to the side of the 1-K box. These plates perform two tasks; they act as thermal anchoring points for the detector wiring, and also help to carry heat away from the 1-K box. The box is constructed from two main sections, bolted together, and this improves the thermal contact to the side of the box opposite the link to the still. Connections from these straps also run to a copper plate near each of the FPUs (e.g. component 12). This provides an all-copper path to the connector plate of each FPU, and is also a mounting location for detector wiring heat sinks.

Links within the subarray modules run from this point to the heat sink for the 1-K electronics modules, which are the dominant source of heating at 1-K within the FPUs. This is described in more detail in section 2 4.

The wiring heat sinks are constructed by sandwiching the ribbon cables between copper plates (with area 90×45 mm^2), and gluing them together with Stycast 2850FT epoxy. The plates are permanently attached to the ribbon cables, and the wires are installed by bolting the plates to corresponding copper plates on the 1-K box. Further heat sinks of a similar design are used at the 4-K and 60-K stages in the instrument.

A further thermal link [4], attached to the main epoxy joint copper plate, is used to provide cooling to the SCUBA-2 shutter [1]. The shutter and its motor operate from the 4 K stage and are outside the scope of this paper; the shutter itself is, however, cooled by the 1-K stage.

The 1-K box is supported from the 4-K stage by CFRP struts. Values are available in the literature for the conductivity of CFRP, but there are many types of CFRP, depending on the nature of the carbon fibres and the matrix in which they are embedded [7]. No values were available for the type we used, and any case there is always the possibility of significant lot-to-lot variations with materials of this type, since the low temperature conductivity is not a parameter of importance to most users of the material. Measurements were therefore made on samples from the actual sheets to be used to make the components in the instrument.

2.3 Millikelvin stage

The millikelvin thermal links have a simpler topology than the 1-K system, with only a single branch between the dilution fridge and the FPUs. However, as is usually the case at such low temperatures, the requirements on the overall conductance are much more demanding. The number of joints was therefore kept to an absolute minimum. As with the 1-K stage, helicoils are used in the tapped holes for all joints, and A2 non-magnetic stainless steel bolts were used.

Their design is complicated by the fact that the links have to be supported but thermally isolated from the 1-K box, and are totally enclosed by shielding at a temperature of approximately 1.5 K. This shielding provides thermal radiation and straylight protection for the detectors, and is a more reliable solution than providing baffling where the millikelvin straps enter the detector units. Light baffles would require parts which were very closely fitting but did not touch since a touch would cause a thermal short from the millikelvin to the 1-K system. This could have been achieved, but was felt to be an unnecessary complication.

A flexible link runs from the mixing chamber of the dilution fridge to a junction on the 1-K box called the "manifold" (component 5 in Fig. 5, and shown in Fig. 7). This link runs in curved flexible bellows (shown in Fig. 2). The construction is similar to the links between the still and the 1-K box, but only two stacks of 50 foils are used. Other differences are that the straps were gold plated throughout, and the welds were not supplemented by bolts since there were no concerns about the weld quality on these straps. Ideally, one end of the link would bolt directly to the mixing chamber. However, to aid assembly, an intermediate plate is bolted permanently to the mixing chamber. The end of the link clamps around a cylinder which protrudes from this plate. This scheme means that the orientation of the insert (which was procured separately from the instrument itself) is not critical. This link is unbolted at the mixing chamber end to remove the 1-K box from the cryostat.

Figure 7: Photograph of the "manifold" in the millikelvin thermal links, showing the Kevlar® wheel support structures. An idea of the scale of this joint can be obtained from the fact that the bolts are M4 size

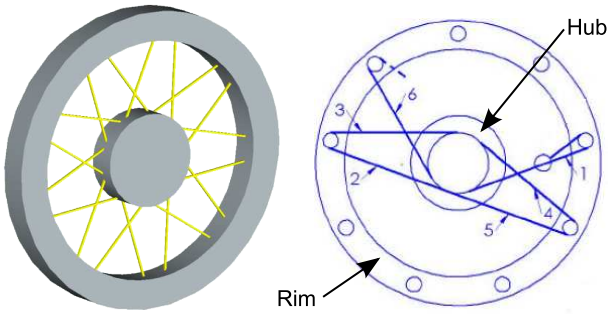

Figure 8: Left: Schematic of the Kevlar wheel assembly used to support the millikelvin straps. Right: diagram showing how the Kevlar is threaded to form the assembly; the thread passes round the numbered points in order.

Since the manifold is mounted on the 1-K box, supports are needed which minimise the heat transferred into the millikelvin system. This is achieved by using supports constructed from Kevlar® in tension. This is a common technique for large cryogenic instruments [8, 9]. Kevlar has a favourable strength/conductance ratio, and when used in tension provides rigid supports with low thermal conductance. Two such supports (called "wheels") are used, since each one only provides constraints in a single direction.

Kevlar *expands* as it is cooled, and also creeps with time; this complicates the design of thermal isolation assemblies using Kevlar, which generally employ a system of pulleys and capstans to maintain tension. In this case, the assembly is not required to provide precise positioning, and we developed a simpler design which was adequate for our purposes. A sketch of the design is shown in Fig. 8. To assemble the wheel, one end of a single length of Kevlar is looped around a screw to hold it. The thread is then passed back and forth between the rim and the hub, running round small posts on the rim, as shown in Fig. 8. This is repeated until the starting point is reached. Tension is maintained for an hour by attaching a 3 kg weight to the free end of the Kevlar; most of the creep will take place dur-

ing this time. Matching parts are then screwed tightly onto the outer ring and hub, trapping the thread in place. The protruding ends of the thread are then removed. The Kevlar running between the rim and hub then consists of 18 sections, each approximately 20 mm long. Apart from two breakages attributed to force applied during handling, assemblies with this design have functioned well here and elsewhere over repeated thermal cycles.

Two links leave the manifold, one to each of the two FPUs. As with the link to the mixing chamber, they run within cylindrical radiation shields, although in this case they are straight. Ideally, these links would bolt directly to the link to the mixing chamber. However, a practical design required all three straps to bolt to the manifold plate, so that there are two interfaces from one link to another. Each interface uses six M4 screws at a torque of 2 Nm. The links from the manifold to the FPUs are actually part of the FPUs, and are described in the next section. To remove an FPU, the links are unbolted at the manifold.

2.4 Focal plane units

The 1-K and millikelvin systems come together in the FPUs, and are both described in this section. Each FPU contains four subarray modules. These can be removed and replaced independently from each other. The design of the subarray modules is not considered to be part of the *instrument* thermal design, and thus is outside the scope of this paper. However, when installed they form an integral part of the FPUs both from a thermal and mechanical point of view, and they are therefore described here in some detail. The FPUs and the sub-array modules contain sections at the mK and 1-K temperature levels. Each module is divided into three parts, as shown in Fig. 1. The connector plate connects to the 1-K circuit board via the detector wiring and a thermal link. The 1-K circuit board connects directly to the millikelvin section only by the detector wiring. The three sections are independently mechanically supported by the FPU. The 1-K sections are bolted to the FPU in several places; thermal contact across these joints is not critical, as they are not required to carry heat. The millikelvin section carries the detector heat sinks. These are bolted to their supports in the FPU. Good thermal conduction across this joint is very important as it is part of the link between the detectors and the dilution fridge.

At the 1-K stage, the FPUs have a thermal path to the still through the structure of the 1-K box. However, the conductance through this path is likely to be relatively poor, and relying on this cooling path alone could cause local heating in the FPUs. Since the heat leak across the supports to the millikelvin stage increases rapidly with increasing temperature at the hot end, this could result in an unacceptable heat leak to the millikelvin stage. The dominant heat load at the 1-K stage is from the electronics on the 1-K PCB in the subarray modules, and an all-copper path is therefore provided between the electronics and the still.

A gold plated ETP copper link (component 26 in Fig. 1) connects the electronics modules to the gold plated copper connector plate on the subarray module. Copper links (component 10 in Fig. 9), run from each connector plate to a split annular link running round the centre of the FPU (component 11). A similar link (not visible in Fig. 9), runs to the 1-K strap system around the 1-K box and thus to the still.

The millikelvin system in the FPUs and subarray modules is more critical. As mentioned above, the links running from the manifold to the FPUs are actually part of the FPUs. To remove an FPU, the joint at the manifold is broken, and as the FPU is withdrawn from the 1-K box the link slides out of the cylindrical radiation shield. No further joints have to be broken apart in the millikelvin system to remove an FPU.

The "U" shaped link, running from locations 4 to 4a in Fig. 1, is made from three lengths of solid ETP copper bar, electron beam welded together. The cross-section of the lengths from 4 to 4b is 25 mm $\times$ 3 mm, and the part from 4a to 4b has a circular

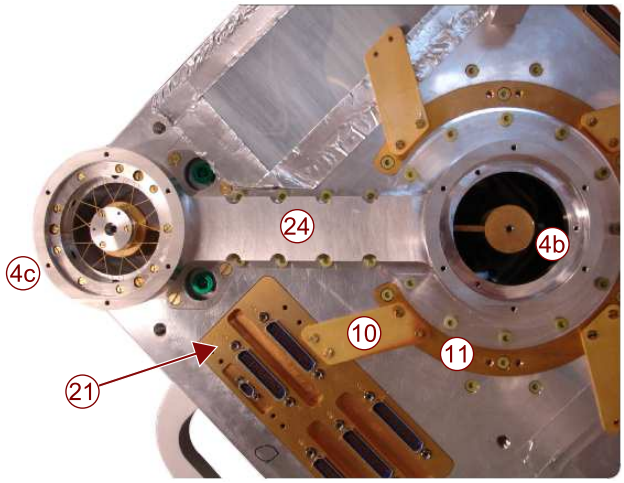

Figure 9: Photograph showing the millikelvin thermal link system in an FPU, along with the 1-K thermal links on the outside of the FPU. The numbered components are: 1-K thermal links (10,11), connector plate (21), the millikelvin thermal link (4b, 4c) and the millikelvin thermal link cover (24).

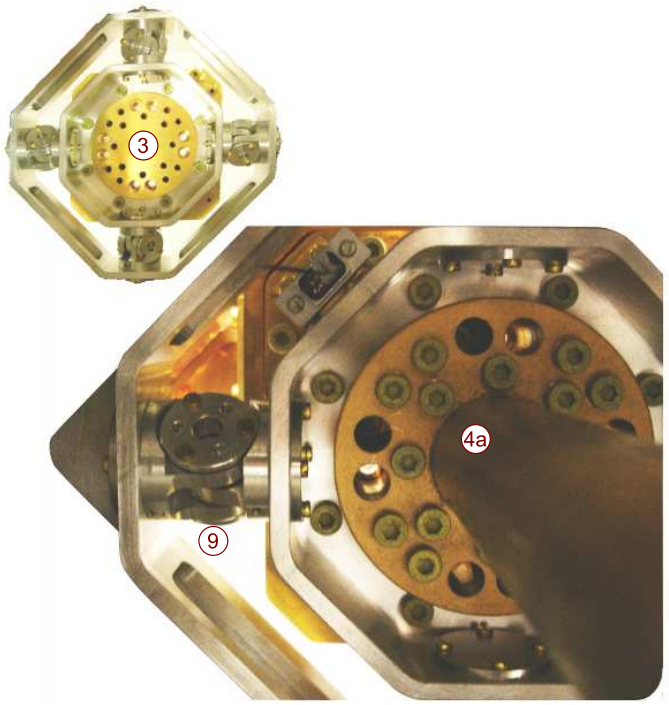

Figure 10: Photograph of the hairbrush support from underneath, showing part of the sapphire thermal isolation support structure. The entire sapphire support is shown in the top left hand corner, without the thermal link installed. The numbered components are: the millikelvin thermal link (4a), a sapphire thermal isolation unit (9) and a hairbrush support (3).

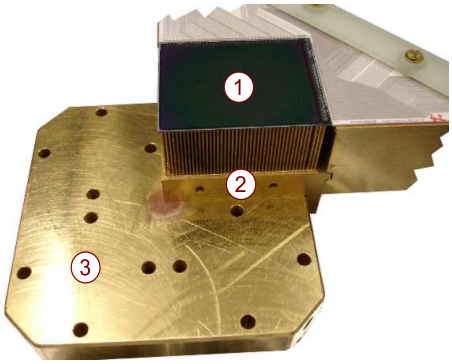

Figure 11: The hairbrush support (3) with a single subarray unit installed. On the subarray unit the detector (1) and the hairbrush (2) are visible. The joint between components 2 and 3 is the interface between the instrument millikelvin subsystem and the subarray modules.

cross-section with diameter 26 mm. The total length is 815 mm (for the 450 μm focal plane). The bar is supported at the corners by Kevlar® assemblies identical to those used at the manifold. Inside the FPU, the link terminates in a circular plate, shown in Fig. 10. This bolts to a platform (the hairbrush support) made from commercial copper (component 3 in Figs. 1 and 11). The bolted joint is made using eight M4 aluminium screws with a torque of 1.7 Nm. Due to the proximity to the detectors, we avoided stainless steel, since even nominally non-magnetic steel may have some residual magnetism.

The hairbrush support is rigidly mounted to the 1-K structure of the FPU. In this case we wished to avoid the use of Kevlar®, due to the possibility of creep over time spoiling the optical alignment, and also the danger of catastrophic failure of the Kevlar® thread. However, there was insufficient space to use a rigid support using a good bulk thermal insulator. The solution was to make use of the poor thermal conductance across a joint between sapphire discs with alumina powder between them [10]. Good thermal isolation is achieved because the two sapphire surfaces are very hard, and only touch at a small number of points, giving a very small true contact area. If a softer material (such as a metal) were used, the surfaces would deform to some extent under pressure, increasing the contact area. The powder decreases the contact area further from that of two sapphire surfaces in direct contact. This provides a rigid structure to support the arrays with a sufficiently low thermal conductance. The open structure allows access to the back of the arrays, enabling the use of bolted joints to the detector heat sinks

A development programme, described in detail in Ref. [11], was carried out to optimise the design of single sapphire-powder-sapphire joints, which to our knowledge have not been used before for this purpose. The full support, shown in the corner of Fig. 10, uses four of these joints to provide a support which is constrained in all three dimensions. A prototype support was constructed; the thermal performance has been measured at operating temperatures, and the mechanical strength has been measured at room temperature. Both were well within the specifications, and the mechanical performance should not be significantly different at lower temperatures.

A second path for heat transfer between the 1-K and millikelvin stages of the FPU occurs via the array wiring in the subarray module. To minimise thermal conductance, ribbon cables were fabricated by depositing niobium tracks onto Kapton® ribbon cables [12]. The hairbrush support connects to the detector heat sinks (component 2 in Figs. 1 and 11). These are generally referred to as the "hairbrushes" due to their appearance. The rationale for their design is as follows. The detectors are made from silicon, and must be heat sunk across the whole surface to carry away the heat generated during operation. The conduction laterally through the silicon is relatively poor, and the detectors would heat beyond their operating temperature if heat was only removed from the edges. Furthermore, uniform heat sinking is required since variation in temperature of the pixels leads to variation in pixel performance across the array. Achieving such heat sinking is difficult because the thermal contraction of silicon is not well matched to metals.

The solution was to fabricate a heat sink consisting of many thin beryllium copper tines, each of which is individually bonded to the detectors [12]. The tines are 22 mm long, and have a cross-section of 0.5×0.5 mm^2. To increase the contact area, the cross-section increases to 0.8×0.8 mm^2 at the tips. The larger cross-section cannot be used throughout as the tines would then not have sufficient flexibility. It is possible to fabricate such a component by electron discharge machining (EDM). Copper would be the ideal material from a thermal point of view, but is not sufficiently elastic. We therefore used a high conductivity beryllium copper alloy (C17500, temper not specified but believed to be TF00). The hairbrushes contain a separate tine corresponding to each pixel in the detector, and the tines are bonded to the silicon with Stycast 1266 epoxy. Once bonded, it is almost impossible to check that each tine is bonded well and that there is no glue bridging the tines, and in any case it is not possible to remove the detector to make a second attempt. The bonding was therefore carried out by using a desktop robot to deposit a metered amount of epoxy separately onto each tine, before placing the detector onto the hairbrush using a jig.

The impact of this on the design of the instrument millikelvin stage is that the final interface is to a beryllium copper surface, not copper, and we are unaware of any previous work on the conductance of such bolted joints The thermal contraction of the two materials is similar (C17500 contains over 96% copper), so differential motion is unlikely to be a problem. However, beryllium copper is much harder than copper, and soft materials make good contact because they can deform so that the two sides conform to each other. We therefore made conductance measurements on a representative joint [11]; these showed that we could achieve suitable performance. The joints between the hairbrushes and the hairbrush support are each made using four M4 aluminium screws with a torque of 1.7 Nm.

3 Modelling and measured performance

The thermal design presented a difficulty common to other complex cryogenic instruments. The ultimate requirement on the thermal performance is that the temperature of the bolometer heat sinks within the silicon detector wafer should reach a specified temperature [13]. However, this is a somewhat indirect requirement for much of the instrument, since the temperature within the detectors depends on the thermal architecture of the detectors themselves as well as the instrument. In order to make the design practical, the instrument was divided into subsystems; these include the detectors themselves as well as the millikelvin and 1-K stages of the instrument. It was necessary to set requirements for each subsystem so that the design

Table I: Power loading on the 1-K stage (in decreasing order of power) [14].

Source	Power (mW)
1-K electronics	0.256
Array wiring	0.163
Shutter and shutter motor	0.088
Supports from 4-K stage	0.054
Radiation	0.0007
Optical radiation	4×10^{-6}

could begin even though the properties of the other subsystems were not yet known. However, keeping to strict requirements which were chosen before the design stage is likely to lead to a non-optimal design.

Our approach was to maintain a model of the entire thermal system, from room temperature to the detectors themselves. Parameters in the model were based on reliable data from the literature where possible. Otherwise, measurements were carried out on representative samples. As described above, these were necessary for the conductance across the copper to beryllium copper joint between the hairbrushes and the hairbrush supports, across the sapphire isolation stage and along the CFRP (carbon fibre reinforced plastic) struts linking the 1-K box with components at higher temperatures [4]. This model was used to set initial requirements for each subsystem, so that the design could begin. The design of each subsystem was fed into the overall model, which was then used to adjust the requirements for the subsystems if necessary to achieve an optimal overall thermal design.

For the millikelvin thermal system, we set a requirement of a maximum temperature difference of 20 mK across the entire thermal link (i.e. between the mixing chamber and the hairbrush supports). For the 1-K stage, there was a strict requirement that the 1-K box be no warmer than 1.5 K, based on the radiative loading on the detectors. However, the conductive loads on the millikelvin stage would be rather high from this temperature. We therefore set the requirement of a maximum temperature of 1.1 K at the wiring heat sinks and at the points where the sapphire support structure was mounted. As the design of the millikelvin stage progressed, we were able to relax this requirement to 1.3 K.

As the detailed *mechanical* design progressed, the thermal models were updated in parallel with changes. In several cases, changes which reduced the thermal performance, such as the addition of extra bolted interfaces, were requested on mechanical grounds. The model was used to determine whether they were acceptable from a thermal point of view.

3.1 1-K stage

The thermal model showed that the requirements for the 1-K system should be met with a considerable amount of margin. Table I shows the predicted power loading on the 1-K stage. There are few thermometers on the 1-K stage, and a detailed comparison with models is therefore not possible.

The temperature of the FPU covers were measured to be below 1.4 K. Since these are extremities of the 1-K box, with thermal contact to the still being via several bolted aluminium joints, this suggests that the overall requirement of a temperature below 1.5 K has been met. Since the other requirements for this stage (a temperature of 1.3 K or lower at the wiring heat sinks and sapphire support stage) were based on the effect on the millikelvin stage, direct temperature measurements are not necessary. However, the temperature at the 1-K box end of the thermal link to the still (component 16 in Figs. 2 and 5) is 1.16 K, suggesting that they were met.

The still temperature was found to be around 1 K, instead of 900 mK as expected. Measurement of the still cooling power suggests that this corresponds to a power loading of approximately 10 mW on the 1-K stage, which is larger than expected. The reason for this is not clear, though there are several potential sources of such heat. It is evident that the detector wiring heat sinks are not perfect. Measurements of the temperature distribution along the wiring have suggested temperatures of 10-20 K at the heat sinks on the 4-K stage. This would result in a larger than expected length of the wires being in the normal (as opposed to superconducting) stage. However, the change in conductivity between the normal and superconducting states is small enough that the effect on the total power loading would not explain the discrepancy. Superconducting wire was chosen for electrical, not thermal properties, and was necessary to reduce Joule heating in the wires at the 1-K stage to an acceptable level. Joule heating is not the cause of the excess power since it is present when the arrays are not powered up. There are many places where structures in the 1-K and 4-K stages are close to each other, and a possible explanation is a thermal short circuit occurring during cool-down. Since the requirements for this stage were met in any case, it has not been necessary to identify and correct this situation.

Table II: Predicted thermal loads on the cryostat fourth (mK) stage. The power loads are divided into the contribution from each focal plane and the contribution of the common sections of the system. The first two rows give the power dissipated in the detectors themselves and the multiplexing electronics respectively [14]. More details are given in the text.

Element	Power (μW)		
	850 μm	450 μm	Common
Detectors (8 subarrays)	0.23	1.02	n/a
MUX (8 subarrays)	2.38	2.83	n/a
Supports	7.4	7.4	0.4
Array wiring (8 subarrays)	2.1	2.1	n/a
Radiation	n/a	n/a	1.4×10^{-4}
Total	12.11	13.36	0.4
Total load		25.89	

3.2 Millikelvin stage

Modelling of the millikelvin stage during the design process showed that the performance was much more critical than the 1-K stage. Thermometry at various locations permits a comparison between the model and the measured values. Ruthenium Oxide thermometers[3] were used, calibrated against a commercial calibrated thermometer.

The predicted thermal loading on the millikelvin system is shown in Table II, and the measured temperature at various

[3] Model RX-102ACD, Lakeshore Cryotronics, Westerville, Ohio, USA

Table III: The predicted and measured temperatures at various points in the millikelvin thermal link system [14]. The component numbers all appear in Fig. 12. For the values predicted with two arrays installed, the mixing chamber temperature was taken at the measured value during operation, and the model of the system was used to obtain the remaining temperatures. For the predicted values for eight arrays, measurements of the dilution refrigerator performance in a test cryostat were used to obtain the expected mixing chamber temperature under the increased power.

Location	Temperature (mK)		
	Two arrays		Eight arrays
	Measured	Predicted	Predicted
450 μm system			
Hairbrush (2)	-	57.4	61.3
Hairbrush support (3)	56.3	57.3	61.3
Link (4) - warm end (4a)	-	57.0	60.7
Link (4) - cold end (4d)	-	56.1	59.5
850 μm system			
Hairbrush	-	57.3	61.1
Hairbrush support	72.9	57.3	61.0
Link - warm end	-	56.9	60.6
Link - cool end	-	56.0	59.5
Combined			
Manifold (5)	55.0	55.7	59.0
Link (6) - warm end (6a)	-	55.0	58.0
Link (6) - cold end (6d)	53.5	54.2	57.0
Bolt plate (7)	-	53.5	55.9
Mixing chamber (8)	52.7	(52.7)	54.8

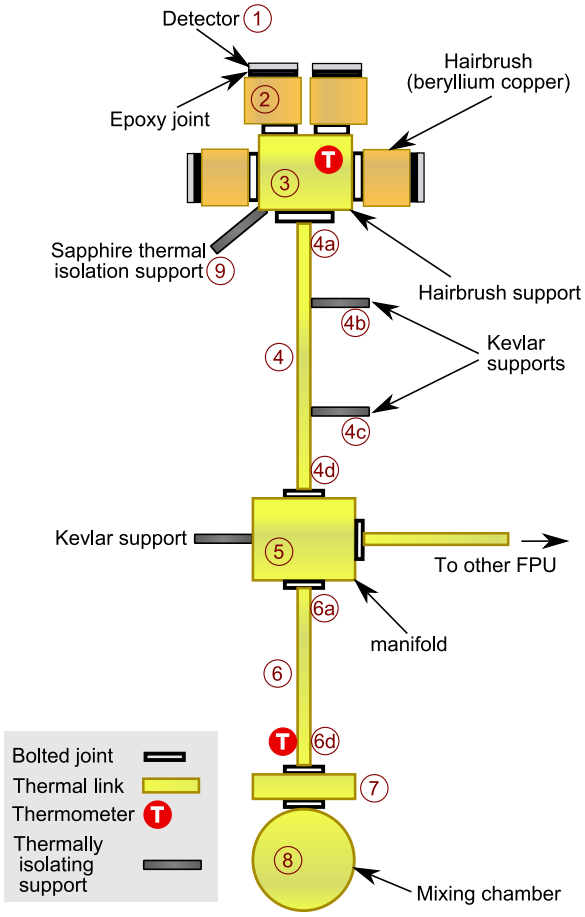

Figure 12: Diagram of the millikelvin thermal link system.

points is shown in Table III. This is compared to predicted values for a configuration with two sub-arrays present (as measured), and for a full complement of eight arrays. The thermal paths are shown in Fig. 12.

Choosing parameters for the model was not straightforward. The conductivity of 5N copper varies greatly depending on the treatment and the source of the copper [15]. We measured samples of the material used for the flexible links, obtaining RRR (residual resistivity ratio [16]) values of over 1400 after annealing. To simplify the measurements, the electrical resistance was measured at a temperature of 4 K, and the thermal conductivity calculated using the Wiedemann-Franz law [16]. Since we did not measure the actual materials used, we added margin to the model by assuming an RRR value of half the measured value. For the ETP copper, we took an RRR of 90, which is the lower limit of values typically found for commercial copper. The hairbrushes are made from C17500 beryllium copper. We are not aware of thermal conductivity measurements on this material at cryogenic temperatures. However, the composition and quoted room temperature conductivity are both similar to C17510, which *has* been measured [17]. Since there is a good correlation between room temperature and cryogenic conductivity of dilute copper alloys [18], we felt justified in assuming the same conductivity as C17510, particularly since the bulk conductivity of the material does not dominate the expected temperature gradient between the arrays and the mixing chamber.

For the bolted joints, again it is hard to predict the performance since there are many parameters which affect the behaviour, and they are not well understood. Even with measurements of the exact configurations used, there is still likely to be large variation between nominally identical joints, and even the same joint after being broken apart and remade. We used a value of $0.4\ T$/K WK^{-1} for the conductance of each copper bolted joint, where T is temperature. This somewhat arbitrary value was obtained by taking the approximate lower value for measurements on bolted joints with somewhat lower torque and fewer bolts [6], then multiplying by a factor of 4 to allow for the increase in expected performance. The temperature variation of conductance across joints was taken to be that of bulk ETP copper, in the absence of any information to the contrary. Values for the conductance of the copper to beryllium-copper joints were taken from our own measurements [11].

A value for the conductance of the sapphire joint thermal isolation structure is required in order to predict the heat leak onto the millikelvin stage; this was taken from measurements on the prototype system [11].

As can be seen from table II, the agreement between the predicted and measured values is generally reasonable. The actual performance is better than the predictions, as might be expected since we used pessimistic values in the model. The exception to this is the hairbrush support in the 850 μm system, which is somewhat warmer than expected. The temperature has varied after removal and replacement of the FPU, suggesting poor performance at a bolted joint. However, we also suspect that there is an error in the calibration of this thermometer.

Running the model for the heat load expected with a full complement of eight arrays shows that the requirement of a 20 mK temperature difference should still be easily met by both systems. However, clearly the model is incorrect for the 850 μm system. While we do not know the source of the unwanted thermal impedance, we can approximate the performance by assuming that the entire temperature difference between the manifold and the hairbrush support occurs at a single joint. The conductance across this joint can be taken from the measured values, assuming (as with the other joints) that it follows the same temperature dependence as ETP copper. Under this assumption, the hairbrush support will reach 81.2 mK with the power loading expected from a full complement of sub-arrays. Although this is greater than the requirement, the detectors will still attain their required performance at this temperature, and therefore it will not be necessary to modify the system even if the high measured temperature is real (as opposed to being due to thermometer calibration error).

4 Conclusions

Despite its complexity, and the need to develop novel techniques, the thermal design of the SCUBA-2 instrument has been extremely successful. In particular, we achieved a temperature difference of under 4 mK for a thermal link across a distance of over 1.5 m and through 5 bolted joints, carrying an (estimated) load of over 10 μW. The thermal design met the requirements on the first cooldown, and has operated in a reproducible manner over eight cooldowns, with the 1-K box and FPUs being removed and replaced between each cooldown. The performance has also remained stable after the instrument was disassembled and transported by air and sea from Scotland to the telescope in Hawai'i. The experience with SCUBA-2 and the new techniques developed can be used to aid the successful design of future instruments with similar or greater complexity.

5 Acknowledgements

We would like to thank Julian House for his help in the preparation of this paper.

[1] Audley MD, Holland WS, Duncan WD, et al. SCUBA-2: A large-format TES array for submillimetre astronomy. Nuclear Instruments and Methods in Physics Research A 2004;520:479.
[2] Gorla P, Ardito R, Arnaboldi C, et al. Cuoricino and CUORE detectors: developing big arrays of large mass bolometers for rare events physics. Nucl. Phys. B (Proc. Suppl.) 2006;150:214.
[3] Woodcraft AL, Ade PAR, Bintley D, et al. Electrical and optical measurements on the first SCUBA-2 prototype 1280 pixel submillimeter superconducting bolometer array. Rev. Sci. Inst. 2007;78:024502.
[4] Gostick D, Montgomery D, Wall B, et al. The cryo-mechanical design of SCUBA-2: a wide-field imager for the James Clerk Maxwell Telescope. Proc. SPIE 2004;5492:1743
[5] Woodcraft AL. Predicting the thermal conductivity of aluminium alloys in the cryogenic to room temperature range. Cryogenics 2005;45:421.
[6] Didschuns I, Woodcraft AL, Bintley D, et al. Thermal conductance measurements of bolted copper to copper joints at sub-Kelvin temperatures. Cryogenics 2004;44:293.
[7] Reed RP, Golda M. Cryogenic composite supports: a review of strap and strut properties. Cryogenics 1997;37:233.
[8] Roach PR. Kevlar support for thermal isolation at low temperatures. Rev. Sci. Inst. 1992;63:3216.
[9] Duband L, Hui L, Lange A. Thermal isolation of large loads at low temperature using Kevlar rope. Cryogenics 1993;33:643.
[10] Yoo KH, Anderson AC. Thermal impedance of pressed contacts at temperatures below 4 K. Cryogenics 1983;23:531.
[11] Bintley D, Woodcraft AL, Gannaway FC. Millikelvin thermal conductance measurements of compact rigid thermal isolation joints using sapphire-sapphire contacts, and of copper and beryllium-copper demountable thermal contacts. Cryogenics 2007;47:333.
[12] Duncan W, Audley D, Holland W, et al. SCUBA-2 arrays to system interfaces. Nuclear Instruments and Methods in Physics Research A 2004; 520:427.
[13] Holland WS, Duncan W, Kelly BD, et al. SCUBA-2: A large format submillimeter imager for the James Clerk Maxwell Telescope. Proc. SPIE 2003;4855:1.
[14] Hollister MI. The SCUBA-2 Instrument: An Application of Large-Format Superconducting Bolometer Arrays for Submillimetre Astronomy. Ph.D. thesis, Edinburgh University, 2009.
[15] Woodcraft AL. Recommended values for the thermal conductivity of aluminium of different purities in the cryogenic to room temperature range, and a comparison with copper. Cryogenics 2005;45:626.
[16] Pobell F. Matter and Methods at Low Temperatures. Springer, 1992.
[17] Woodcraft A, Sudiwala RV, Bhatia RS. The thermal conductivity of C17510 beryllium-copper alloy below 1 K. Cryogenics 2001;41:603.
[18] Woodcraft AL. Zirconium copper - a new material for use at low temperatures? In Y Takano, SP Hershfield, SO Hill, PJ Hirschfeld, AM Goldman, editors, Low Temperature Physics: 24th International Conference on Low Temperature Physics - LT24, volume CP850. American Institute of Physics, 2006; pp. 1691–1692